ANALYSIS OF TAIL ROTOR NOISE REDUCTION BENEFITS USING HELINOVI AEROACOUSTIC MAIN/TAIL ROTOR TEST AND POST-TEST PREDICTION RESULTS

J. Yin, A. Dummel[1], D. Falchero[2], M. Pidd[3], J. Prospathopoulos[4], A.Visingardi[5], S.G. Voutsinas[4]

Deutsches Zentrum für Luft- und Raumfahrt (DLR), Germany
e-mail: jianping.yin@dlr.de

[1] EUROCOPTER (ECD), Germany
e-mail: Andreas.Dummel@eurocopter.com

[2] EUROCOPTER (ECF), France
e-mail: Daniele.Falchero@eurocopter.com

[3] QinetiQ, United Kingdom
e-mail: mpidd@QinetiQ.com

[4] National Technical University of Athens (NTUA), Greece
e-mail: jprosp@fluid.mech.ntua.gr; spyros@fluid.mech.ntua.gr

[5] Centro Italiano Ricerche Aerospaziali(CIRA), Italy
e-mail: a.visingardi@cira.it

Key words: Helicopter tail rotor noise reduction, Main/Tail Rotor Interaction, HELINOVI Aeroacoustic Test, Numerical Simulation

Abstract: The EU HeliNOVI project was designed to improve the understanding of Tail Rotor (TR) noise reduction and vibration reduction technology by means of a comprehensive investigation of Main Rotor (MR)/TR interaction noise and rotor induced vibrations through both theory and experiment. Several tail rotor noise reduction techniques were investigated both through wind tunnel testing and through simulations. The investigation included tip speed reduction, the sense of TR rotational direction and different TR rotor position. Both the test and simulation results indicate that tail rotor noise is most important for climb and high-speed level flight. The analysis of the tail rotor noise reduction benefits from test and simulation results show that besides a reduction of rotor tip speed, the most efficient tail rotor noise reduction concept consists in changing the tail rotor sense of rotation from 'Advancing Side Down-ASD' to 'Advancing Side Up-ASU'. In addition, the noise reduction for new TR position is mainly due to increasing the advancing blade distance rather than changing TR aerodynamic behavior.

1 INTRODUCTION

Helicopter noise reduction is a long term objective of the helicopter industry in view of extending the market to new civil applications, as well as getting prepared to comply with new and increasingly stringent noise regulation. The main sources of helicopter noise are its main rotor (MR), tail rotor (TR), engine, and the drive-train components. The dominant noise contributors are the MR and the TR since they operate in free atmosphere and thus radiate noise unobstructed into the surroundings.

The main research effort in the past was concentrated on the reduction of MR noise, where extensive work, both theoretical and experimental has helped to deepen the understanding of the mechanisms of the generation and reduction of MR noise such as recent work reported in [1]. Even though the TR has long been recognized as a significant source of helicopter noise [2~7], there has been little research effort towards tail rotor noise reduction. The reason is that the complex flow surrounding the TR poses an extreme challenge for both experimental and theoretical study.

The EU HeliNOVI project was designed to resolve this deficiency in TR noise research and is part of the continuing EU effort towards improving the understanding of TR noise reduction and vibration reduction technology by means of a comprehensive investigation of MR/TR interaction noise and rotor induced vibrations through both theory and experiment. The general description and some preliminary test results can be found in [8~10].

As regards the experimental part of the HeliNOVI project, a comprehensive wind tunnel test campaign was launched. The test model is a 40% scaled BO105 helicopter model with instrumented main/tail rotor and fuselage. The importance of tail rotor and of main / tail rotor interference noise as well as of tail rotor noise reduction potentials is investigated in detail. The tested configurations involved in the test are BO105 main rotor (MR) and tail rotor (TR) in combined and isolated conditions. In addition, a number of noise reduction techniques are tested;

(1) TR sense of rotation (NACA 0012 TR used),
(2) Variation of position between MR and TR (S102 TR used),
(3) Variation of rotor rotational speed.

As regards the theoretical part of the HeliNOVI project, five codes of varying complexity from 6 organizations (CIRA, DLR, ECD, ECF, NTUA and QinetiQ) were used in producing the pre/post-test data base of numerical results plus flight mechanics codes for determining the control angles. The adaptation and validation of reliable prediction tools, with reference to the new experiment data set as well as numerical simulations on noise reduction techniques were conducted. The flight conditions covered included level, climb, and descent flight at various flight speeds.

The objectives of this paper are to analyze the effect of several TR noise reduction techniques on helicopter noise reduction. The analysis is conducted by using both the test and prediction results and focuses on the comparison between the results produced by both test and numerical simulations. The investigation includes tip speed reduction, changing the sense of TR rotational direction and different TR rotor position. The experiment results used in analysis contain (1) inflow microphone measurements, and (2) unsteady blade pressure. The noise reduction benefits are discussed.

2. DESCRIPTION OF TEST AND THEORETICAL SIMULATIONS

2.1 Brief description of the test system

HeliNOVI wind tunnel test campaign was performed in DNW 8m by 6m open jet test section known for its excellent flow quality and anechoic properties as well as its low background noise. *Fig. 1* presents an overview of the test set up and DLR test rig as well as inflow and outflow microphone system in this wind tunnel.

Fig. 1: HeliNOVI test set up for aeroacoustic test

The BO105 model consists of dynamically and Mach scaled main rotor blades and a geometrically scaled fuselage including teetering tail rotor system. The model is well equipped with densely instrumented MR (NACA23012 airfoil) and TR (S102 airfoil; NACA0012 airfoil) as well as a lightly instrumented fuselage. To improve the understanding of the effect of MR wake on TR inflow, a 3-component flow visualization and flow velocity measurement, by means of Particle Image Velocimetry (PIV), are also employed on planes near TR inflow and outflow region parallel to the free stream. The acoustic signal is measured by the inflow microphone array (16 Mics) mounted on a traverse. Besides the conventional measurement techniques, a 140-microphone out-of-flow phased array was applied to locate and quantify the different noise sources on the model. The rotational speed ratio between the TR and the MR was set to 5:1 for the HeliNOVI test campaign.

2.1 Brief description of the numerical simulation

The numerical simulations in this report are performed by 6 EU partners including two airframe manufacturers with 5 codes of varying complexity. All codes are formulated within the context of the potential flow theory and the associated integral equation methods that can be derived. Compressibility effects are taken into account basically by applying Glauert's correction. As regards noise evaluation, all codes are based on the Ffowcs-Williams Hawking's acoustic analogy theory as detailed in Farassat's formulations. In acoustic computations the quadrupole term has been neglected. The main characteristics of the codes are summarized in the following table.

Table 1: Main Characteristics of the aerodynamic codes

	P3	P4	P1&2	P6	P5
Flow	Direct BEM	Indirect BEM	Lifting Line	Indirect BEM	Lifting Line
Kutta	Pressure	Flow aligning	-	Pressure	-
Wake	Panels	Panels	Vortex Filam.	Vortex Blobs	Vortex Filam.
Ma effects	Glauert/ Full Pot.	Glauert		Glauert/ Euler	Glauert/ Full Pot.
Re effects	-	-	-	2D VI	
Dynamics	-	-	Yes	Yes	Yes

Codes from partner P3, P4 & P6 are based on 3D free wake panel method while partner P1 & 2 and P5 consist of a chain of interconnected modules both having a lifting-line free wake aerodynamic model of the MR and TR systems as their basic component. P3 is using the direct integral formulation (the flow within the solid bodies is set to stagnation) while P4 & P6 the indirect formulation of the Hess type. P3 & 6 use the Kutta pressure condition in order to determine the blade loading while in P4 the flow at the wake panels in contact with the blade is aligned with the wake surface which is in consistency with the dipole distribution over the mean surface of the blade. Compressibility effects are taken into account basically by applying Glauert's correction. In addition, P3 and P5 have the option to use the incompressible baseline flow computation as input to a full potential compressible code while P6 uses instead an Euler solver in a section-by-section procedure. The wake is represented in the form of connected vortex filaments except for P6 which applies a vortex blob approximation of the wake. Regarding other worth mentioning features of the codes, a) P1&2, 5 and 6 are capable of performing coupled aeroelastic computations, b) P6 has the option to extend vorticity emission over the blade tip and c) P6 has the option to include viscous effects by means of strong viscous-inviscid interaction. In general, the force trim according to trimmed data from the test is used except P3 maintained the average value of both MR and TR thrust coefficients equal to the experimental ones through adjusting the collective pitch values.

A detailed description of different aerodynamic and acoustic code as well as the code validation can be found in [11, 12, and 13]

3. RESULTS AND DISCUSSION

The organization of this chapter is as follows. Section 3.1 discusses the importance of TR noise in the standard configuration. In Section 3.2 the effect of different TR noise reduction concepts are analyzed. In all computations, only thickness and loading noise have been considered. It should be mentioned here that the correctness of the prediction on loading noise is strongly dependent on correctness of the prediction on blade surface pressure.

3.1 Main rotor (MR) and Tail rotor (TR) noise contribution at standard configuration

Test results

For a global overview of the contribution of MR and TR to the overall helicopter noise, the mean dBA value is used. The mean dBA value is defined here by averaging over measured area or over all microphone positions, as shown in *Fig. 2*. The mean dBA value as a function

of typical flight condition is given in *Fig. 3*. The comparison for two different TR rotors (one with S102 profile and the other with NACA0012 profile) is also given in the plot.

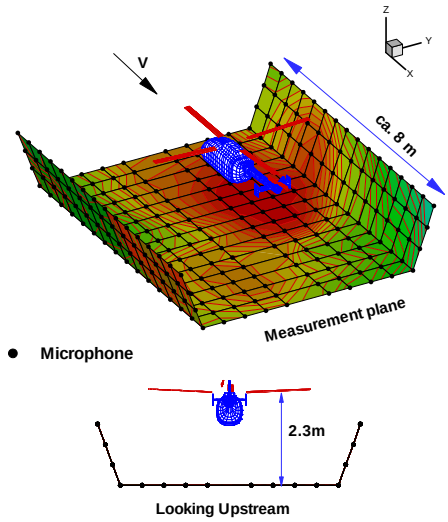

Fig. 2 Measurement plane and microphone positions

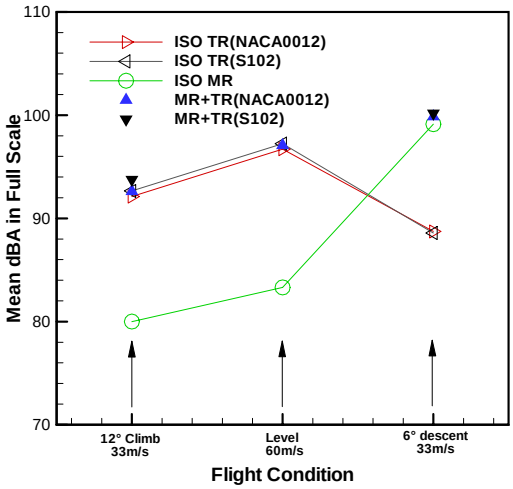

Fig. 3 Mean dBA value as a function of typical flight condition and MR/TR configurations

In general, following points can be drawn from *Fig. 3*:

1. The TR is major source of noise at 12° climb with 33m/s flight speed and 60m/s level flight whilst the MR dominates total noise radiation during 6° descent flight in which MR BVI noise occurs;
2. The comparison of noise level for MR/TR operation with that for isolated TR show a slightly increased noise level for MR/TR operation of both NACA0012 (0.5dBA for 12° Climb) and S102 (1.1dBA for 12° Climb at 33m/s flight speed);
3. The mean noise level is slight higher for TR with S102 profile;
4. The small increment of TR noise level in MR/TR combined condition in comparison with isolated TR condition seems to indicate the effect of the MR wake on the TR noise noticeable but may be secondary.

From acoustic test result analysis, it can be stated that:

1. The benefit of overall noise reduction in climb and level flight is dependent on TR noise reduction; and
2. The benefit of overall noise reduction in descent flight is dependent on MR BVI noise reduction.

Simulation results

The full validations of the aerodynamic and acoustic code are given in [12, 13]. The numerical validation shows the general tendency of MR/TR noise contribution to overall noise is captured by the partners. In this section, selective comparisons with measurements are presented. Two cases are chosen. The first one is the 6° descent flight at 33m/s in which MR is main source of noise; the second case is 60m/s level flight in which TR is main source of noise.

Fig. 4 left compare post-test predictions with measurements for 6° descent flight in terms of the MR normal force time variation at the 87% radial station and MR Cp chordwise distribu-

tion at selected time. MR BVI at both advancing and retreating side was captured and compared quite well with test results not only in position but also in magnitude. *Fig. 4* right compare overall noise contour plot with measurement in terms of full-scale dBA on the plane defined in *Fig. 2*. The acoustic result shows both the maximum noise level and noise directivity are captured by the predictions. Due to weak contribution of the TR, the TR noise does not show up in the plot.

Fig. 5 left compare post-test predictions with measurements for 12° climb flight in terms of the TR normal force time variation at the 80% radial station and TR Cp chordwise distribution at selected time. Good correlation between the simulation and DNW test is observed.

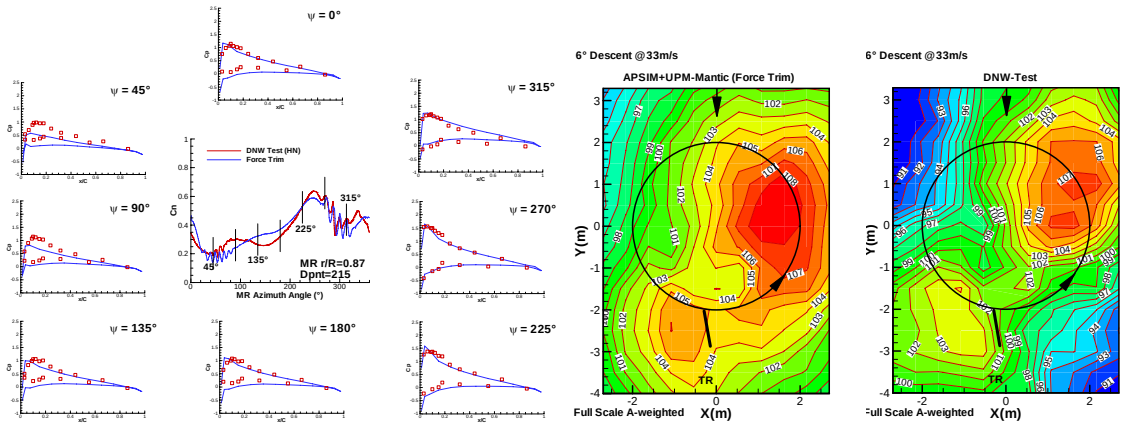

Main Rotor (MR) Cp and Cn Full Scale dBA Contour (left: test)

Fig. 4 Cp and Cn time history and noise contour for 6° descent flight

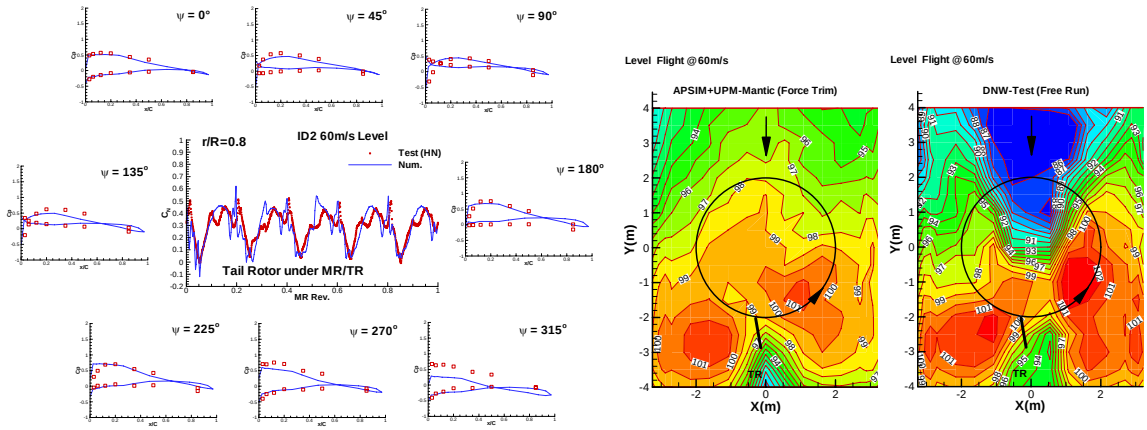

Tai Rotor (TR) Cp and Cn Full Scale dBA Contour (left: test)

Fig. 5 Cp and Cn time history and noise contour for 12° climb flight

3.2 Tail rotor noise reduction potential evaluation

An important aspect of the EU HeliNOVI project was to assess the acoustic benefit in view of realistic helicopter operation and to eventually establish design guidelines for future less noisy helicopters with conventional tail rotors. An assessment of the TR noise reduction potential through variation of blade tip speed, change of the TR sense of rotation, and modification of the TR position is presented in the following sections.

3.2.1 Change TR rotational direction

Previous TR noise research found that it is desirable for TR to rotate Advancing Side Down (ASD) to minimize the interactions with ground and "wingtip" vortices as well as TR noise. The original BO105 TR is already rotated in Advancing Side Down direction. In order to verify whether this preferable TR rotational direction is a general rule for TR noise reduction, the test is conducted by changing TR rotational direction from ASD to Advancing Side Up (ASU), as shown in *Fig. 6*. The TR with a NACA0012 profile is used in this test.

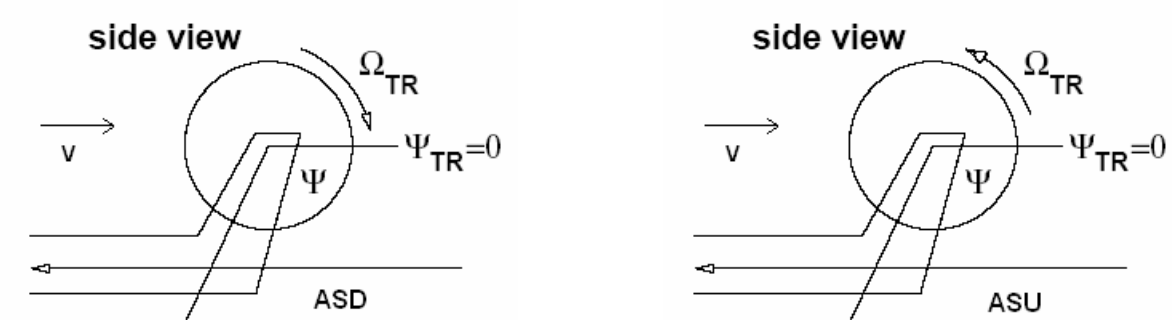

Fig. 6: Different TR rotational direction (Circle represents TR disk), left: Advancing Side Down (ASD); right: Advancing Side Up (ASU)

In general, TR rotor performance such as rotor thrust has a major effect on TR noise radiation. In order to verify this noise reduction found by reversing TR sense of rotation is not caused by changing either TR or MR performance, the TR and MR performance data for both ASU and ASD rotational mode are compared. The variations in performance for TR in ASD & ASU modes are negligible.

Representative Aeroacoustic and Aerodynamic results (test)

The mean dBA value as a function of 3 different flight conditions is given in *Fig. 7* for two different TR rotational directions; ASD & ASU. When compared to TR in ASD mode, a noise reduction of more than 5 dBA is observed for the 12º climb and 60m/s level flight conditions in ASU mode. There is no change in overall noise radiation for 6° descent where MR BVI noise is the dominant noise source.

It is obvious that one factor affecting TR noise reduction is the increased distance from the source located in advancing blade to the observers (microphones) when TR is rotating in ASU mode. The maximum noise reduction due to increasing the advancing blade distance can be estimated as 2.7dB for 12° climb and 2.3 dB for level flight by assuming a source localized at 80% radial position of TR. By making a distance correction to the noise reduction with above mentioned maximum value, a conservative noise reduction due to the change of TR aerodynamic behaviour and of radiated noise directivity can be estimated (marked as distance corrected value (black line with gradient symbol) in *Fig. 7*). There is no change for 6° descent because the MR BVI noise dominates.

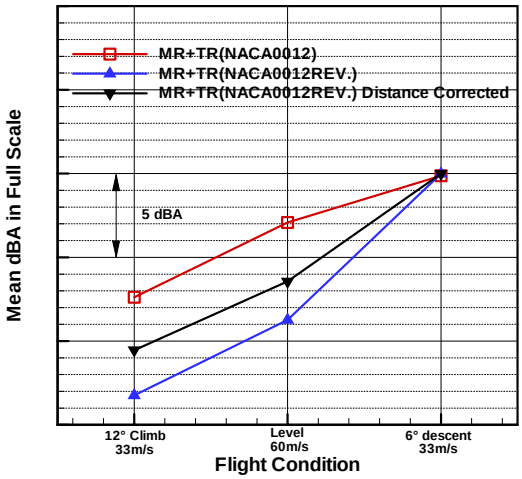

Fig. 7: Mean dBA value as a function of typical flight condition for TR in ASD & ASU mode

The influence of the direction of TR rotation on TR noise can also be demonstrated more in detail by observing noise contour plots as shown in *Fig. 8* for two different flight conditions at 12° climb and 60m/s level flight. The comparisons show that the noise reduction, at the maximum noise area marked, is about 8 dBA for the 12° climb case (*Fig. 8a*) and about 6dBA for 60m/s level flight condition (*Fig. 8b*). The contour plots show the maximum noise area in ASU TR mode has shifted upstream. The shifting is due to the higher source position on advancing side in ASU TR mode.

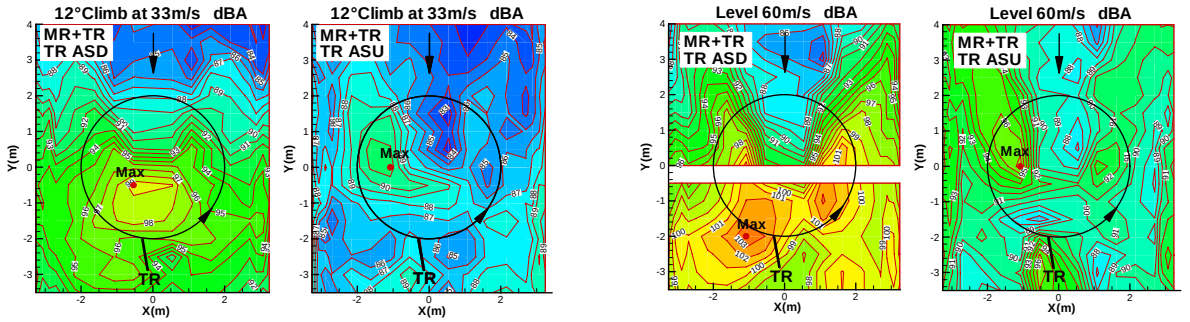

(a) 12° Climb at 33m/s, TR equipped with NACA0012

(b) 60m/s Level flight, TR equipped with NACA0012

Fig. 8: Comparison of full scale dBA contours for the combined operation of both MR and TR in different flight conditions and TR rotational direction

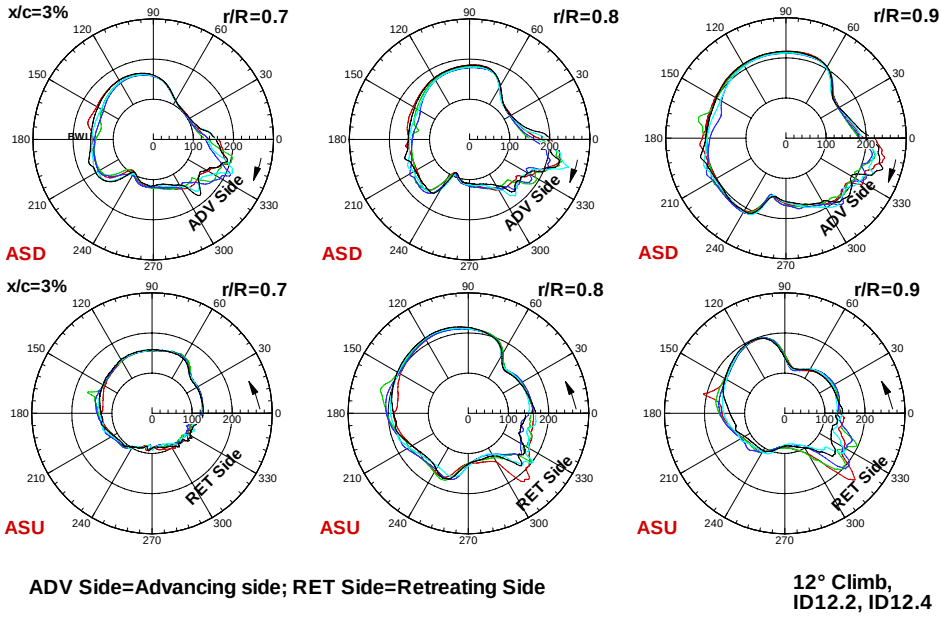

Fig. 9: Polar directivity of TR blade pressure on upper surface in –Kpa for 12° climb

From the Ffowcs-Williams Hawking's acoustic analogy theory, loading noise is strongly dependent on unsteady blade surface pressure. The TR blade pressure is shown in *Fig. 9* as polar plots for a general overview on the variation of Cp at 12° climb. The radius and radiation line in the plot represent a measure of the pressure amplitude and the azimuth angle respectively. TR upper side blade pressure near the leading edge at 3% chord of different spanwise locations in ASD mode are compared with TR in ASU mode. Since the tail rotor flow field varies from revolution to revolution, it is therefore necessary to analyze the data from many revolutions. Each curve in the plot represents TR blade pressure time histories in one TR revolution and results of 5 continuing TR revolutions are given. The arrows in the plots represent the TR rotational direction.

The comparison of polar directivity of blade pressure in ASD and ASU mode shows more clearly that:
In TR ASD mode (upper part of *Fig. 9*), there are BVI like peaks observed on the advancing side (ADV) of TR rotor disk. The BVI peaks occurred for every TR revolution, but the magnitude and phase of each peak varied with the revolutions due to fact that TR inflow field varied from revolution to revolution caused by MR/TR interaction. The blade (MR) wake interaction (BWI) is observed as TR approaches the MR disc (about 180°) from below, but the magnitude of the peak is relatively weak.

In TR ASU mode (lower part of *Fig. 9*), there are obviously BVI peaks occurring on the retreating side of rotor disk, but the magnitude becomes weak for the section moving inside. The magnitude and phase change with TR revolutions. A strong blade (MR) wake interaction (BWI) is noticed in the form of a TR Cp jump as it approaches the MR disc from above, but only for certain TR revolution. There is no BVI like peaks observed on the advancing side of TR rotor disk, indicated by the arrow.

Although in ASU mode, there are some BVI peak occurring on the retreating side of TR rotor disk, from an acoustics point of view the interactions on the advancing side as occurred in ASD mode are dominant due to the locally higher Mach numbers and to the noise directivity downwards. The TR noise reduction in ASU mode is beneficial for lack of BVI on the advancing side as the BVI noise on the retreating side is radiated upwards. Moreover, the scat-

tering effect of the fuselage on the thickness noise is more important in ASU mode. It has been stated that TR noise is dominant source of noise for 12°climb flight condition. Therefore the reduction of overall noise in ASU TR mode is the consequence of TR noise reduction. Similar behavior of the blade pressure is also observed for 60m/s level flight condition in which TR is dominant source of noise too.

Representative Aeroacoustic and Aerodynamic results (numerical simulation)

From acoustic analogy theory, noise radiated from helicopter rotor can be classified as summary of 3 different source terms, (1) loading noise which can be defined by unsteady blade pressure on the blade surface, (2) thickness noise which can be defined by purely kinematics and geometry of the blade and (3) quadrupole noise. For potential flow, as considered here, the quadrupole noise is negligible for low speed flight condition, and therefore is not considered in following numerical results. The advantage of using numerical results is each noise source can be observed independently. The test case was simulated by the HeliNovi partners for 60m/s case and for 12° climb case. Numerical simulation results show that the dominant source of noise for these two flight conditions is TR noise. Therefore, only results from TR are presented although the simulations were done for both MR and TR in operation. The predictions have been performed with force trim according to trim data from the test.

12° Climb Flight at 33m/s (ID12.2 and ID12.4)

The TR's acoustic contribution represented as thickness noise, loading noise and total noise under MR+TR configuration for two different sense of TR rotation are demonstrated in the noise contour plots in *Fig. 10*.

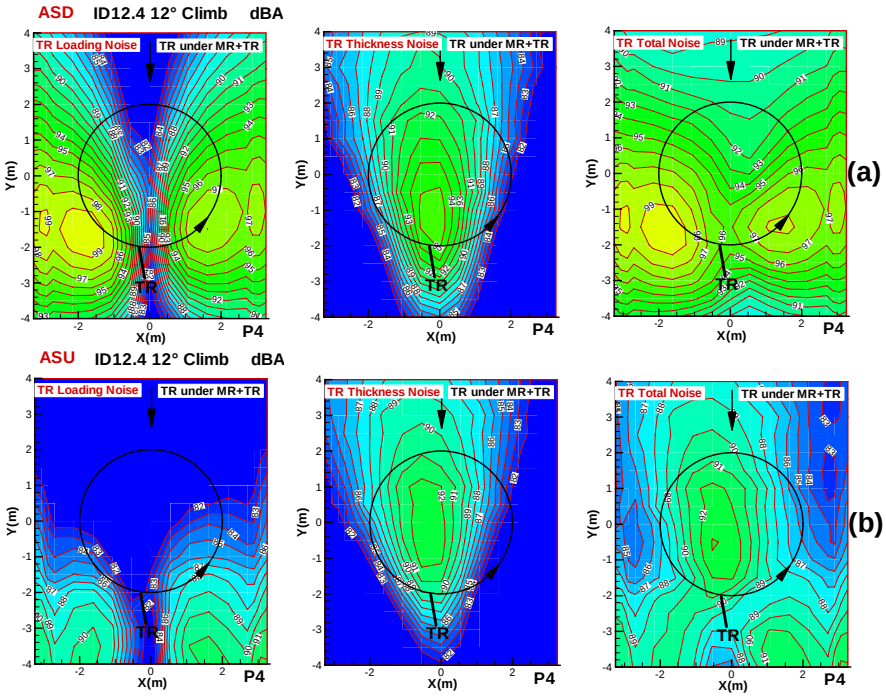

Fig. 10: TR noise under MR+TR configuration in TR ASD (a:upper) and ASU (b:lower) mode (partner P4)

For both TR ASD and ASU rotational direction, TR loading noise is the dominate source of noise along both sides of the tail rotor rotational plane while the TR thickness noise shows a symmetric pattern with the maximum area directly in the tail rotor rotational plane. When comparing with the results of ASD TR mode, TR loading noise level for TR ASU mode is

dramatically reduced and maximum area is shifted further downstream. The maximum area of the TR thickness noise is slightly shifted upstream and magnitude of new maximum area is reduced. As the reduction of TR loading noise in ASU mode, the contribution of TR thickness noise to overall TR noise given in *Fig. 10* (b, right) becomes evident. This characteristic is also observed in the measurement results as shown in *Fig. 8* (a, right), but less evident because of the effect of the shadowing and scattering from the fuselage.

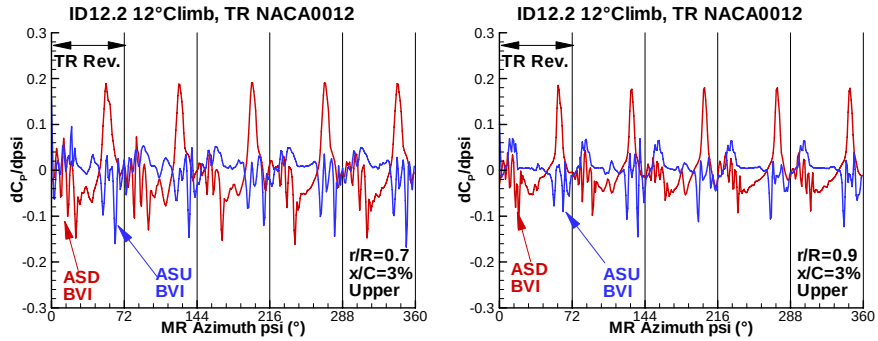

Fig. 11: time gradient of the blade pressure time history of the TR blade leading edge (upper and lower side at 3%) for the two turning modes

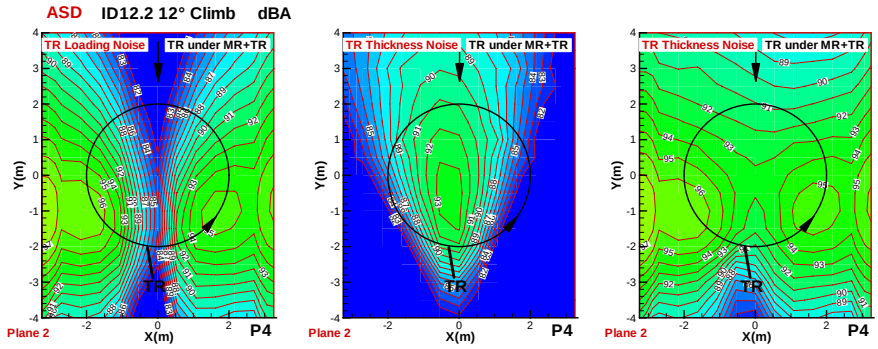

Fig. 12 Predicted TR noise on the plane above the TR in TR ASD (Partner P4)

The reasons for the reduction of TR noise are mainly twofold. First, lack of strong BVI in advancing blade side in ASU mode is observed when comparing with that occurs in ASD mode. *Fig. 11* gives an example of time gradient of the blade pressure time history of the TR blade leading edge for the two TR turning modes. There are obviously BVI peaks occurring on the retreating side of rotor disk in ASU mode, but from an acoustics point of view the interactions on the advancing side as occurred in ASD mode are dominant due to the locally higher Mach numbers. Second, the Mach number of the source in the observer direction is different for the same observer in ASD and ASU mode. It is obviously that the less noise is observed at the observers upstream in ASU mode, because the Doppler amplification factor is less than unity for a receding subsonic source. Therefore TR radiates less noise in upstream direction. In addition, increasing the advancing blade distance in ASU mode will reduce TR thickness noise and shift the peak upstream. In order to estimate the effect of changing the Mach number of the source in the observer direction, the TR noise in ASD mode is again predicted for the observer positions above the TR at the same distance as shown in *Fig. 12*. The comparison of predicted TR noise underneath (*Fig. 10*a) and above (*Fig. 12*) the TR shows the reduction of maximum TR noise is about 3 dBA. This value is much less than the value 7dBA obtained from *Fig. 10*.

In general, the TR noise reduction in ASU mode is beneficial for lack of BVI in advancing side. A 4.18 dBA reduction of mean dBA value is simulated by changing TR sense of rotation from ASD to ASU in comparison with 5.8 dBA reduction from DNW test.

Level Flight 60m/s (ID13.2 and ID13.4)

In this section, both the TR noise represented as thickness noise and loading noise and total noise (MR+TR) under MR+TR configuration for two different sense of TR rotation are demonstrated. The results predicted by different partners are compared and analyzed.

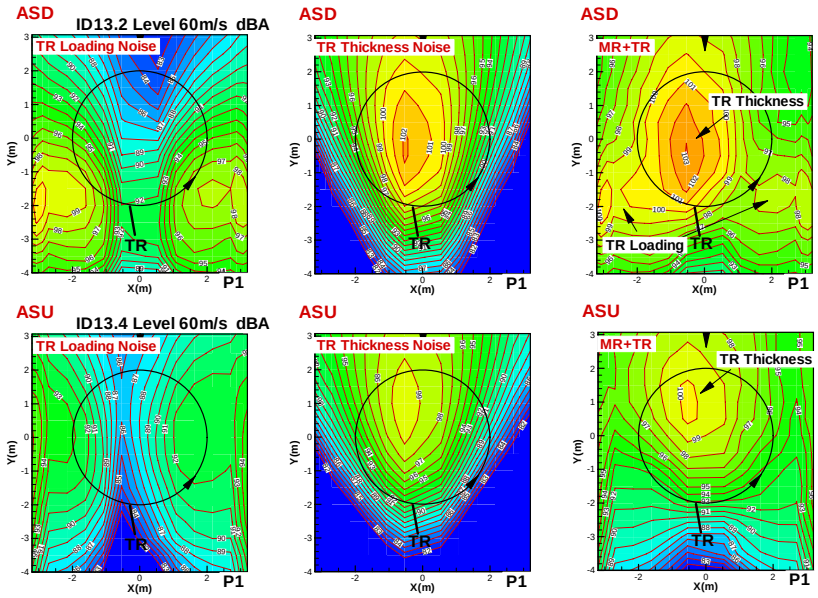

Fig. 13 TR and overall noise under MR+TR configuration in TR ASD and ASU mode (Partner P1)

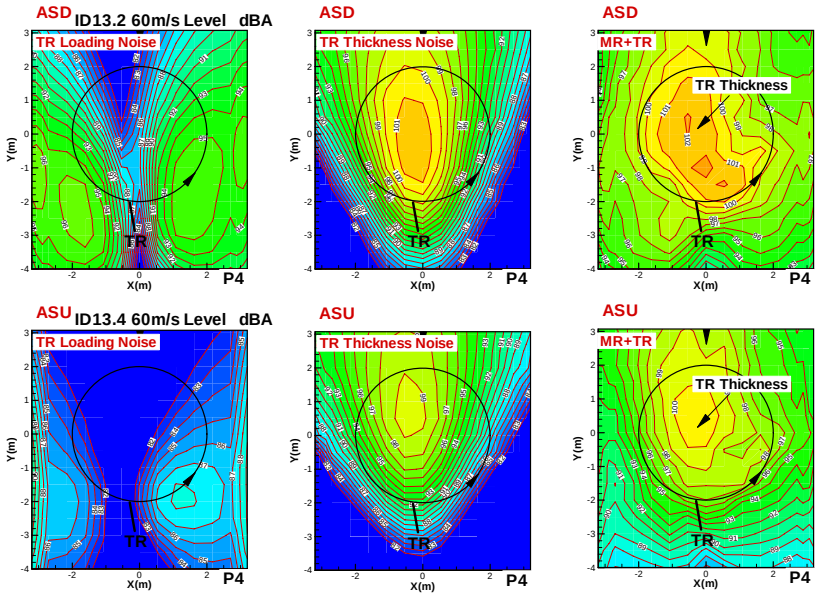

Fig. 14 TR and overall noise under MR+TR configuration in TR ASD and ASU mode (Partner P4)

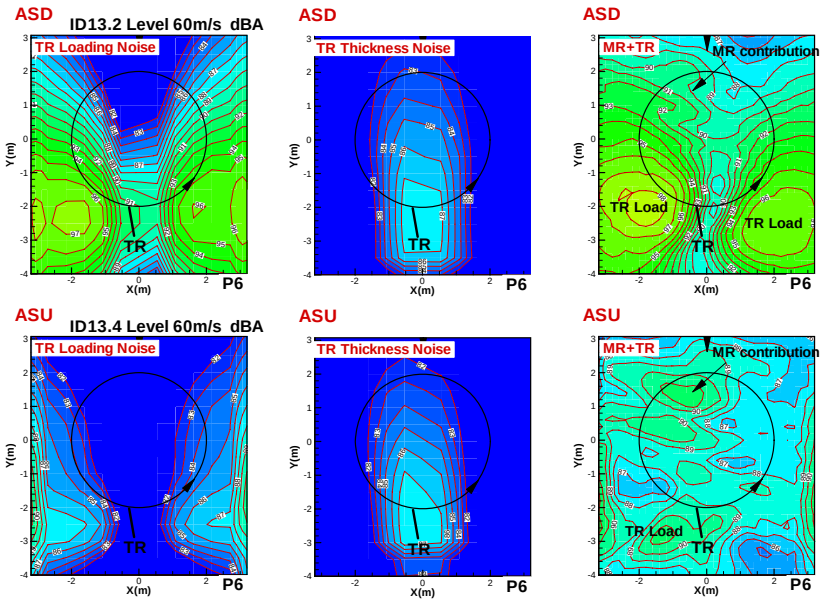

Fig. 15 TR and overall noise under MR+TR configuration in TR ASD and ASU mode (Partner P6)

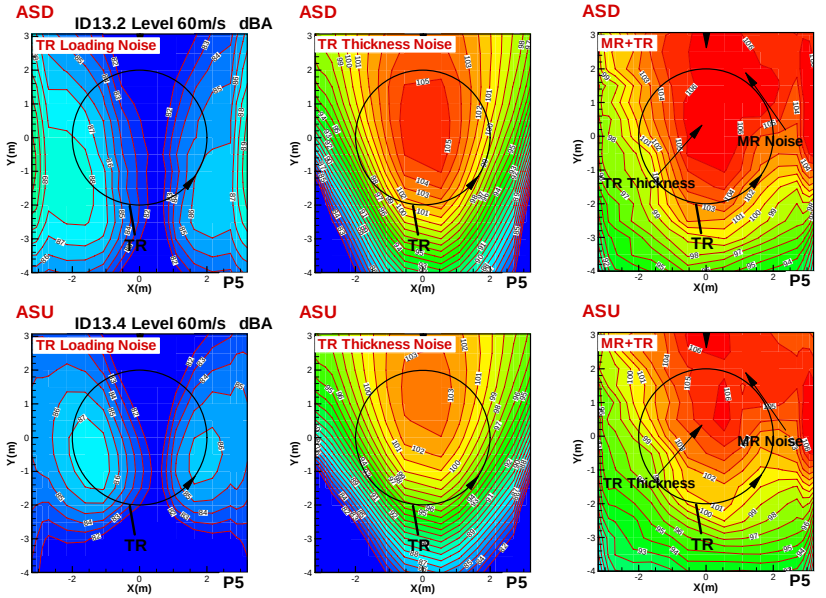

Fig. 16 TR and overall noise under MR+TR configuration in TR ASD and ASU mode (Partner P5)

In general, for both TR ASD and ASU rotational direction, TR loading noise is the dominate source of noise along both sides of the tail rotor rotational plane while the TR thickness noise shows a symmetric pattern with the maximum area directly in the tail rotor rotational plane.

The results in terms of noise directivity from partner P1 (*Fig. 13*) and P4 (*Fig. 14*) are similar. The TR noise contour plot predicted by both partners in ASU mode (lower part of *Fig. 13* and *Fig. 14*) shows similar noise directivity behaviour as for ASD TR mode (upper part of *Fig. 13* and *Fig. 14*) except the loading noise level is dramatically reduced and slightly shifted downstream in P4 results. The thickness noise reduction in ASU mode is owing to the increased distance of the main source only as the effect of fuselage is not considered. The maximum area of both the TR thickness noise and loading noise is slightly shifted upstream. The overall noise contour plots show that in both ASD (upper right) and ASU (lower right) TR mode the maximum noise area is upstream the tail rotor rotational plane, which coincides with charac-

teristics of TR thickness noise contribution. The reversing TR sense of rotation into ASU mode has dramatic reduction in the area along both sides of the tail rotor rotational plane, namely TR loading noise and slightly decreasing TR thickness noise level in TR rotational plane.

Partner P6 results (*Fig. 15*) show potential noise reduction when changing TR sense of rotation from ASD to ASU mode. TR loading noise is dominant noise source. The maximum value of TR thickness noise is much lower than that of TR loading noise. This behaviour is quite different from partner P1 and P4 results in which TR thickness is higher.The overall noise reduction is caused by the reduction of TR loading noise. Emerging of MR loading noise in ASU overall contours shows that further noise reduction can only be achieved if MR loading noise can be reduced. The change of noise directivity is observed due to change of TR sense of rotation.

Partner P5 results (*Fig. 16*) show that the magnitude of TR loading noise is much lower than TR thickness in both ASD and ASU TR mode. Therefore the contribution to the overall noise is negligible. The slightly decreasing overall noise level as shown in *Fig. 16* in TR rotational plane in TR ASU mode is believed to large advancing blade distance to the central microphones than in normal sense of rotation which causes reduction of TR thickness noise. In both ASD and ASU mode, MR noise plays an important role in the overall noise contour.

Following table demonstrates the noise reduction achieved from the experiment and numerical simulation by changing TR sense of rotation from ASD to ASU. The difference of the mean dBA value is summarized. A positive value indicates the achievement of a reduction in the noise.

	DNW Test	P5	P6	P1	P4
60m/s, Level flight	6.1 dBA	1.2 dBA	8.5 dBA	2.9 dBA	2.3 dBA

Summary from partner P5, P6, P1 and P4 numerical simulations:
The partners, P5, P6, P1 and P4, demonstrate the noise reductions when changing TR rotational direction from ASD to ASU. Partner P6 shows the reduction of TR loading noise is the main cause of the reduction of overall noise, while partner P4 and P1 show although TR thickness noise is dominant source of noise, TR loading noise reduction has also contribute to the overall noise reduction. The P5 results show that the cause of overall noise reduction is the reduction of the TR thickness noise.

3.2.2 Lower tip speeds

It is well known that the overall sound level is related to the blade tip speed and therefore a certain noise reduction was expected to occur due to the reduced blade tip speed of MR and TR. A tip speed reduction of about 10% for both MR and TR was tested. The rotors were trimmed in order to keep the same thrust as that at the nominal tip speed. The thrust reduction resulting from a reduced tip velocity was compensated by increasing the blade collective pitch.

Representative Aeroacoustic and Aerodynamic results (test)

The mean dBA value as a function of 3 different flight conditions is given in *Fig. 17* for nominal and reduced tip speed. *Fig. 17* indicates that in general the rotors at reduced tip speed are indeed quieter than with the original tip speed for all the flight conditions tested because the noise radiation is proportional to the rotor tip speed. The influence of reducing rotor tip

speed is particularly highlighted in terms of noise contour plots as shown in *Fig. 18*. As a result of TR tip speed reduction, the beneficial effect on reducing the thickness noise is clearly observed for 12° climb flight condition (*Fig. 18* left) in which TR is dominant source of noise. In this flight condition the maximum noise area is shifted from the thickness noise dominated area (around TR rotational plane shown in *Fig. 18* up-left) to the TR loading noise dominated area along both sides of the tail rotor rotational plane. In addition, the maximum value of TR loading noise has also been reduced of about 3dBA. The reduction of MR BVI noise, especially on the retreating side area at 6° descent (*Fig. 18* Right), is obvious. Therefore it is concluded that reducing tip speed is a most effective way to reduce noise.

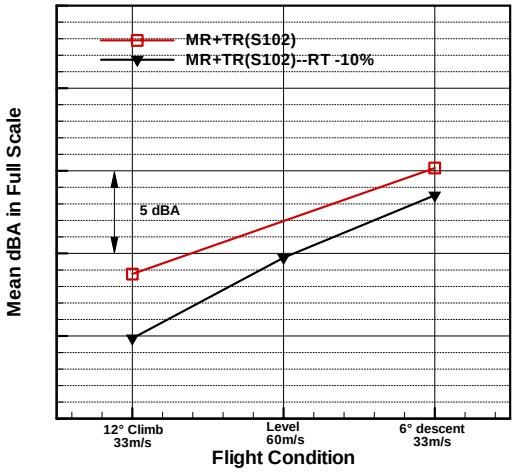

Fig. 17: Mean dBA value as a function of typical flight condition, Effect of tip speed reduction

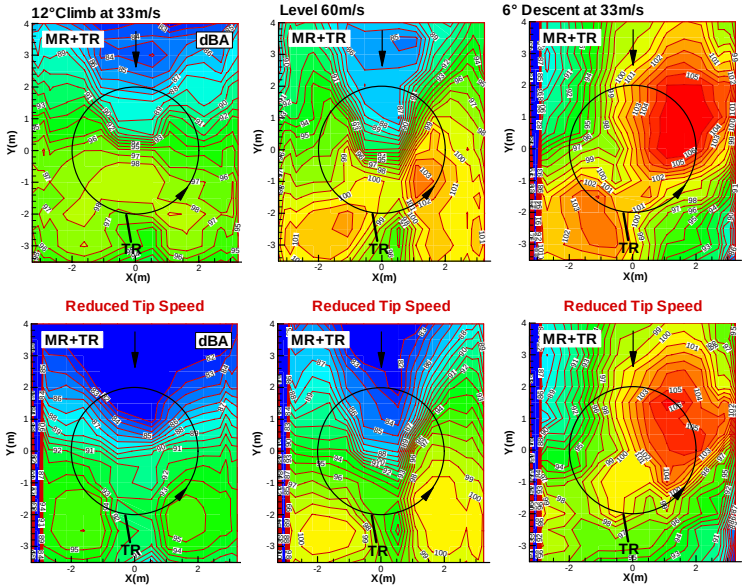

Fig. 18: Noise contour plots at three typical flight conditions, Effect of tip speed reduction

Representative Aeroacoustic and Aerodynamic results (numerical simulation)

Level Flight 60m/s (ID10)

The test case was simulated by Partner P3, P4 and P2. The TR acoustic contribution represented as thickness and loading noise under MR+TR configuration are demonstrated separately in *Fig. 19-Fig. 20*. The comparison of overall noise contour (full scale dBA) with test results in the case of reduced tip speed is given in *Fig. 21*. *Fig. 22* illustrates the comparison with the results of nominal rotor tip speed (ID2).

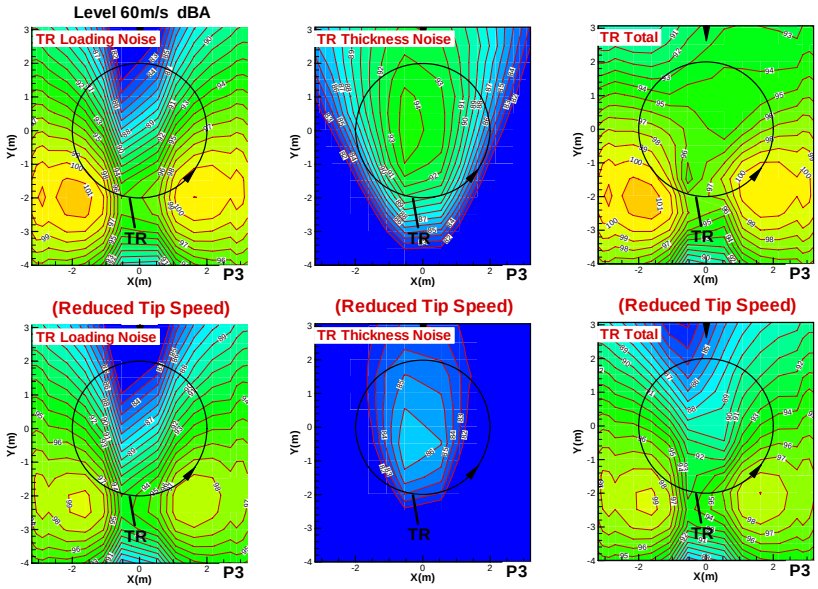

Fig. 19: TR noise under MR+TR configuration for nominal and reduced tip speed (Partner P3)

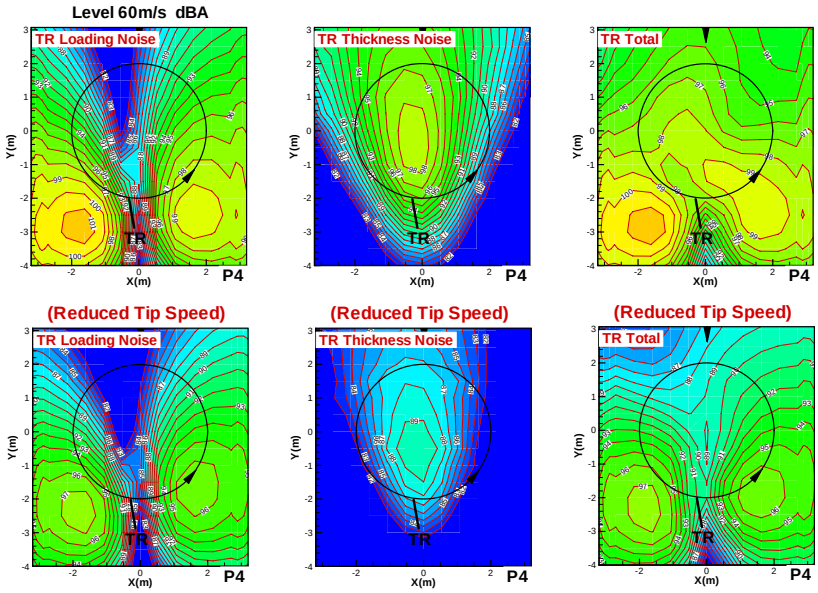

Fig. 20: TR noise under MR+TR configuration for nominal and reduced tip speed (Partner P4)

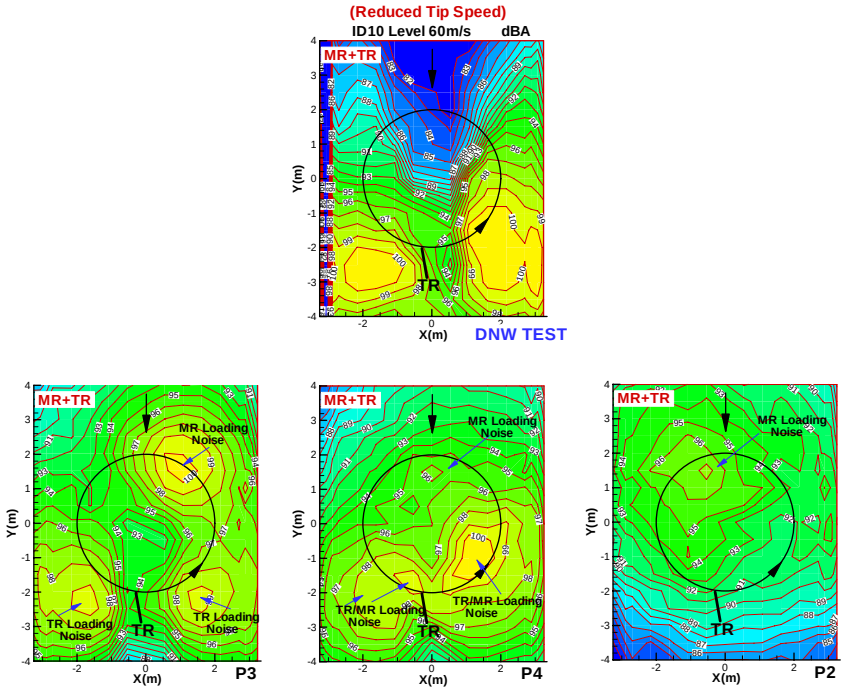

Fig. 21: Comparison of tested and predicted overall (MR+TR) noise contours for reduced tip speed (Test result (up), Partner P3, P4 and P2 Simulation (low))

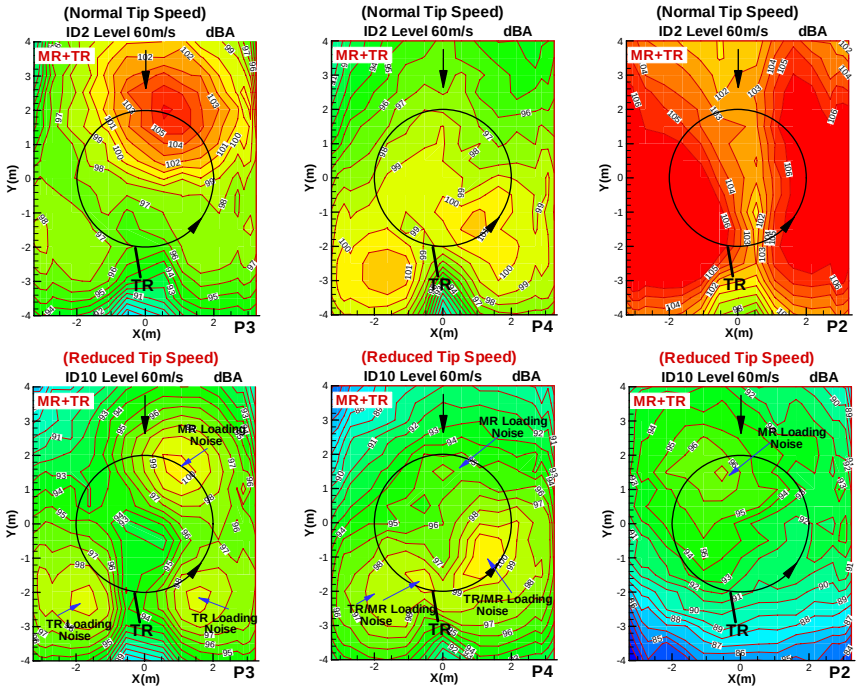

Fig. 22: Comparison of predicted overall (MR+TR) noise contours (nominal tip speed (up), reduced tip speed (low)) (Partner P3, P4 and P2 Simulation)

By comparing *Fig. 19* and *Fig. 20*, TR loading and thickness noise bear a similar directivity pattern for both partner P3 and P4 simulations. TR loading noise contributes to the area along both sides of the TR rotational plane, while TR thickness noise gives a symmetric pattern with the maximum area directly in the tail rotor rotational plane and shows less intensive in maximum value in comparison with TR loading noise. The TR loading noise from partner P4 is slightly lower than that of partner P3 whereas the TR thickness noise for partner P4 is slightly

higher. The reducing tip speed has more influence on the magnitude of TR loading and thickness noise rather than noise directivity.

In partner P3 simulation, the overall (MR+TR) noise contours in reduced tip speed (*Fig. 21*, lower left) display three dominant noise 'hot spots'. The two noise 'hot spots' in the downstream are obviously from TR loading noise and match with experiment result (*Fig. 21*, up), while the third noise 'hot spot' produced by MR loading noise does not show up in the test result. Therefore MR loading noise may be overestimated. The comparison of (MR+TR) noise contours in both reduced tip speed (*Fig. 22*, lower left) and nominal tip speed (*Fig. 22*, upper left) shows a significant reduction in MR loading noise and the appearance of more defined TR "hot spots" which are in close agreement with the experiment.

In partner P4 simulation, the overall (MR+TR) noise contours in reduced tip speed (*Fig. 21*, lower middle) demonstrates the two noise 'hot spots' which are in close agreement with the experiment result (*Fig. 21*, up). These two noise 'hot spots' coincides with characteristics of TR loading noise contribution as shown in *Fig. 19*, left. The comparison of (MR+TR) noise contours from reduced tip speed (*Fig. 22*, middle low) with the result of nominal rotor tip speed (*Fig. 22*, middle, up) shows a clearly reduction of TR noise.

In partner P2 simulation (*Fig. 22*, right above) indicates TR loading noise is dominant noise in the normal rotational speed, while these two noise 'hot spots' does not show up in *Fig. 22*, right lower which indicates the dramatic reduction of TR loading noise. Due to lower level of TR noise in the case of reduced tip speed, MR loading noise can be identified.

The following table demonstrates the noise reduction achieved from the experiment and numerical simulation by reducing rotor tip speed in 10%.

	DNW Test	P3	P4	P2
60m/s, Level flight	2.3 dBA	3.0 dBA	2.5 dBA	13.1 dBA

Summary from partner P3, P4 and P2 numerical simulations:
Although all partners, partner P3, P4 and P2, show a noise reduction when the rotor rotational speed is reduced, partner P3 results show that the reduction of MR loading noise is the main cause of the reduction of the overall noise with a slight increase in the TR loading noise, while partner P4 and P2 results show that the reduction of the rotor tip speed can have beneficial for both MR and TR noise reduction. Furthermore, with reference to the directivity patterns, partner P3 and P4 results are closer to experiment although they both predict a MR hot spot which is more pronounced in P3 simulation.

3.2.3 Change TR Position

The TR location relative to the MR and helicopter operating conditions are two major factors that determine the vortex trajectories on the TR disk. The noise benefit resulting from a change in TR offset in the vertical direction position (to minimize or avoid the interaction with the main rotor wake) is quantified. *Fig. 23* illustrates new TR position with respect to original TR position.

Representative Aeroacoustic and Aerodynamic results (test)

Fig. 24 gives the mean dBA value as a function of 3 different flight conditions for new TR position and compares with that for the original TR position. A distance correction to the

noise reduction as discussed in 3.2.1 is again applied. The results demonstrate that the noise reduction for new TR position is mainly due to increasing the advancing blade distance rather than changing TR aerodynamic behavior.

The noise contours over the measured area are given in *Fig. 25* for 12° climb and 60m/s level flight conditions. When comparing with the results from normal BO105 TR position as shown in upper left part of *Fig. 25* for 12° climb condition, the contour plots show a slight shift of the maximum noise area in the upstream direction due to the high source position of TR advancing side. The decreasing of thickness and loading noise level is observed.

Fig. 26 illustrates the comparison of blade pressure time histories as function of TR revolution and the TR position in 60m/s level flight condition. Each curve in the plot represents TR blade pressure time histories in one TR revolution and the results of 5 continuing TR revolutions are given.

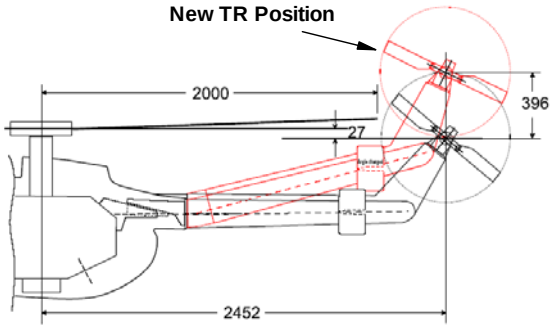

Fig. 23 Drawing of new TR position with respect to original TR position

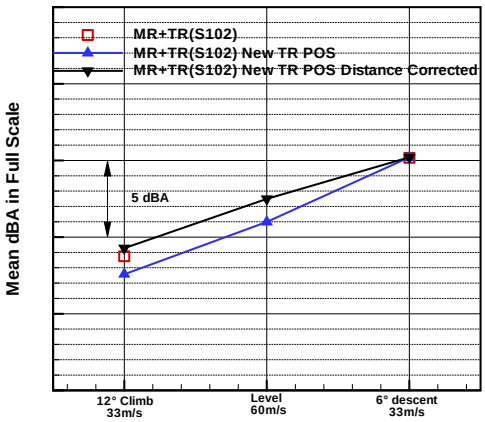

Fig. 24 Mean dBA value as a function of typical flight condition for TR in original and new position

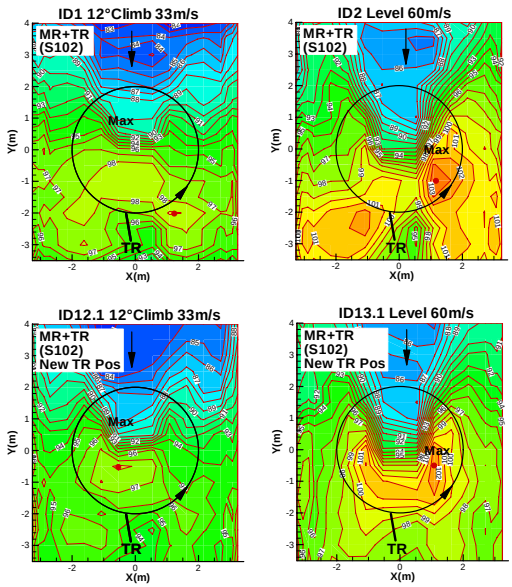

Fig. 25: the noise contours over measured area for 12° climb-and 60m/s level- flight condition at new TR position

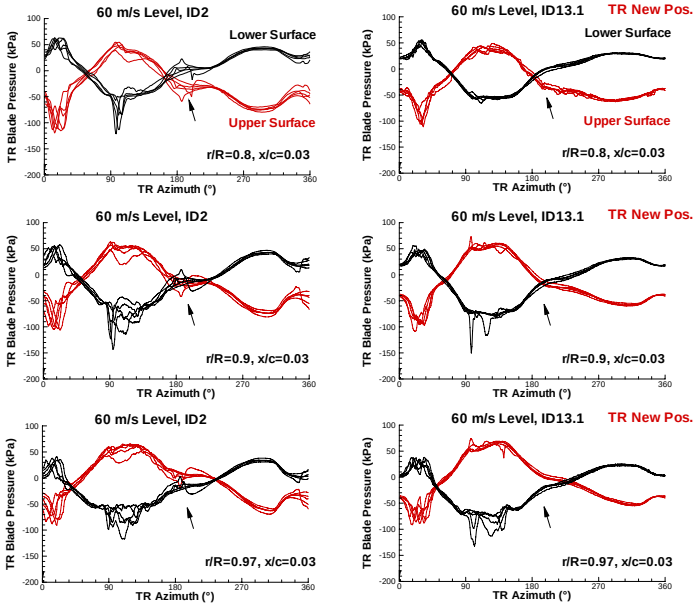

Fig. 26: the comparison of leading edge blade pressure time history as function of TR revolutions for the combined operation of MR and TR in different TR position, Level flight at 60m/s. Left: Normal TR Pos., Right: New TR Pos.

In general, TR blade pressure variations among different TR revolutions decrease for TR blade azimuth angle below 90° when the TR shifted to a new position. The interaction peaks (named as i1, pointed with arrow) occurred around TR azimuth at 180° which is the closets position to the MR rotor disk, dramatically decreased because of increased miss-distance of the TR blade to the MR rotor disk. The interaction peaks (named as i2) occurred in the area between 90° and 140° of TR azimuth angle where the fin is located as shown in *Fig. 26* are believed to be effect of the fin on the development of MR/TR wake. The new TR position has reduced this type of interactions (i2). The type i2 interactions are relative weak for 12° climb flight condition. The reduction of TR loading noise in the area besides the TR rotational plane as shown in the lower part of the *Fig. 25* are the consequence of the weaker interactions (type i1 and i2) for TR in new position.

Representative Aeroacoustic results (numerical simulation)

The test case was simulated by partner P6 and P5 for 60m/s level flight case. The predictions have been performed with force trim according to trimmed data from the test. Both partner observed the slightly decreasing TR loading and thickness noise in new TR position which is mainly due to the fact that the advancing blade of the tail rotor is at a larger distance to the microphones than in normal TR position. Both partners predict no TR noise reduction benefits as shown in following table

	DNW Test	P6	P5
60m/s, Level flight	1.0 dBA	-0.1 dBA	-0.2 dBA

4. CONCLUSIONS

Noise Reduction Benefits from analysis of test results

Besides a reduction of rotor tip speed, the most efficient tail rotor noise reduction concept consists in changing the tail rotor sense of rotation from 'Advancing Side Down-ASD' to 'Advancing Side Up-ASU'. When comparing with TR in ASD mode, a noise reduction of more than 5 dBA is observed for the 12º climb and 60m/s level flight conditions. The noise reduction for new TR position is mainly due to increasing the advancing blade distance rather than changing TR aerodynamic behavior;

The reduction of the overall noise in ASU TR mode is the consequence of reducing the TR loading noise and the TR loading noise reduction in ASU mode is beneficial for lack of BVI on the advancing side;

An averaged noise reduction of 2.7 dBA for the 12º climb and of 2.3 dBA at 60m/s level flight conditions can be achieved by changing the TR rotational direction from ASD to ASU mode;

A maximum noise reduction of about 8 dBA for the 12° climb case and of about 6dBA for 60m/s level flight condition can be obtained. No TR performance penalty is observed by reversing TR sense of rotation.

Noise Reduction Benefits from analysis of numerical results

Prediction of TR noise reduction benefits still challenge task. Although in most of cases, the noise reduction benefits which were observed in the test and were also simulated, the explanation of noise reduction mechanism varied from the partners. This reveals that aerodynamic simulations are crucial to the prediction of the noise.

1. ASD to ASU:

60m/s Level flight:
The partners, P5, P6, P4 and P3, demonstrate the noise reductions when changing TR rotational direction from ASD to ASU. The partners P6 shows the TR loading noise reduction is the main cause of the reduction of overall noise, while P4 and P1 show that although TR thickness noise is dominant source of noise in the TR rotational plane, TR loading noise reduction in the area along both sides of the tail rotor rotational plane has also contributes to the overall noise reduction. The partner P5 results show that the causes of overall noise reduction are the reduction of the TR thickness noise.

33m/s 12° Climb flight:
The partner P4 results show potential noise reduction when changing TR sense of rotation from ASD to ASU mode; TR loading noise is dominant noise source. The overall noise reduction is caused by the reduction of TR loading noise. Emerging of MR loading noise in ASU overall contours shows that further noise reduction can only be achieved if MR loading noise can be reduced.

2. Reduced Tip Speed

60m/s Level flight:
The partner P3 results show that the reduction of the MR loading noise is the main cause of reduction of the overall noise with a slight increase in the TR loading noise, while the partner

P4 and P2 results show that reducing the rotor tip speed can have a positive impact on both MR and TR noise reduction.

3. Change TR position

60m/s Level flight:
The partner P5 and P6 predicted no TR noise reduction benefits.

ACKNOWLEDGEMENT

The HeliNovi project is generously supported by the European Union under the Competitive and Sustainable Growth Programme in the 5th Framework, Contract Nr. G4RD-CT-2001-40113. Special thanks go to the engineers, technicians, and mechanics of DLR, DNW and NLR for their tireless efforts in preparation and conduction of this highly complex test.

REFERENCE

[1] Y. Yu, "The HART II Test - Rotor Wakes and Aeroacoustics with Higher-Harmonic Pitch Control (HHC) Inputs-The Joint German/ French/Dutch/US Project–", 58th Annual Forum of the American Helicopter Society, Montreal, Canada, 2002.
[2] J.W. Leverton, J.S. Pollard and C.R. Willis, "Main Rotor-Wake/ Tail Rotor Interaction", Vertica, Vol.1, pp. 213-224, 1977.
[3] J.W. Leverton, "Reduction of Helicopter Noise by Use of a Quiet Tail Rotor", Paper No. 24, European Rotorcraft Forum, Sept. 1980.
[4] K.-J. Schultz, W.R. Splettstoesser, "Helicopter Main Rotor/ Tail Rotor Noise Radiation Characteristics from Scaled Model Rotor Experiments in the DNW", 49th AHS Annual Forum, St. Louis, Missouri, May 19-21, 1993.
[5] J. Fitzgerald, and F. Kohlepp, "Research Investigation of Helicopter Main Rotor/Tail Rotor Interaction Noise", NASA CR 4143, May 1988.
[6] R.M. Martin, C.L. Burley, "Acoustic Test of a Model Rotor and Tail Rotor, Results for the Isolated Rotors and Combined Cofiguration", NASA TM 101550, Feb. 1989.
[7] A.R. George, and S.T. Chou, "A Comparative Study of Tail Rotor Noise Mechanisms", 41st AHS Annual Forum, Fort Worth, Texas, May 1985.
[8] H.-J. Langer, O. Dieterich, S. Oerlemans , O. Schneider, B. v.d. Wall, J. Yin, "The EU HeliNOVI Project -Wind Tunnel Investigations for Noise and Vibration Reduction", 31st European Rotorcraft Forum, Florence, Italy, 2005
[9] Dieterich , A. Visingardi, H.-J. Langer, G. Imbert, M. Hounjet, S. Voutsinas, I. Cafarelli, R. Calvo, C. Clerc, K. Pengel, "HeliNOVI - Current Vibration Research Activities"; 31st European Rotorcraft Forum; FIRENZE, Italy; Sept. 13-15, 2005
[10] J. Yin, B. Van der Wall, S. Oerlemans, "Representative Test results from HELINOVI Aeroacoustic Main Rotor/Tail Rotor/Fuselage Test in DNW"; 31st European Rotorcraft Forum; FIRENZE, Italy; Sept. 13-15, 2005
[11] S.G. Voutsinas, A. Visingardi, J. Yin, G. Arnaud, D. Falchero, A. Dummel, M. Pidd, J. Prospathopoulos, "Aerodynamic Interference in Full Helicopter Configurations and Assessment of Noise Emission: Pre-Test Modelling Activities for the Helinovi Experimental Campaign". European Rotorcraft Forum, 31st ERF 2005, P68, Florence ,Italy, 13-15, Sep. 2005.
[12] A. Visingardi, A. Dummel, D. Falchero, M. Pidd, S.G. Voutsinas, J. Yin, "Aerodynamic interference in full helicopter configurations: validation using the HeliNOVI database"; 32nd European Rotorcraft Forum; 12 – 14 September 2006, Maastricht, The Netherlands.

[13] M. Pidd, A. Dummel, M. Genito, D. Falchero, John Prospathopoulos, A. Visingardi, S.G. Voutsinas, J. Yin, “Validation of aeroacoustic predictions using the HeliNOVI database”, 32nd European Rotorcraft Forum; 12 – 14 September 2006, Maastricht, The Netherlands.